Slovak University of Technology in Bratislava
Faculty of Chemical and Food Technology
Institute of Information Engineering, Automation and Mathematics

---

Ing. Ayush Sharma

MATHEMATICAL MODELING AND OPTIMAL OPERATION OF MEMBRANE PROCESSES

Doctoral thesis statement

for obtaining the academic title
philosophiae doctor

in the branch of study:
5.2.14 Automation

of the Ph.D. program:
Process control

Supervisor:
Prof. Ing. Miroslav Fikar, DrSc.

Bratislava 2019

The doctoral thesis was completed in a part-time manner of doctoral study at the Institute of Information Engineering, Automation, and Mathematics, Slovak University of Technology in Bratislava.

Candidate: Ing. Ayush Sharma
Inst. of Inf. Eng., Automation, and Mathematics
Slovak University of Technology
Radlinského 9, 812 37 Bratislava, Slovakia

Supervisor: Prof. Ing. Miroslav Fikar, DrSc.
Inst. of Inf. Eng., Automation, and Mathematics
Slovak University of Technology
Radlinského 9, 812 37 Bratislava, Slovakia

Opponents: Doc. Ing. Alena Kozáková, PhD.
Institute of Automotive Mechatronics
Slovak University of Technology
Ilkovičova 3, 812 19 Bratislava, Slovakia

Prof. Jan van Impe, PhD.
Chemical & Biochemical Process Technology & Control
KU Leuven
Gebroeders De Smetstraat 1, 9000 Gent, Belgium

The doctoral thesis statement was distributed on: ....., 2019

The defense of the doctoral thesis will be held on the .... 2019 at ...00 before the Board for Defense of Doctoral Theses in the branch of study:

5.2.14 Automation

at the Faculty of Chemical and Food Technology, Slovak University of Technology Bratislava, room 641 (6th floor, new building), Radlinského 9, 812 37 Bratislava.

doc. Ing. Michal Kvasnica, PhD.
Chairman of the Board for Defense of Doctoral Thesis
Slovak University of Technology
Radlinského 9, 812 37 Bratislava, Slovakia

Contents

Abstract

The objective of this thesis is to mathematically model batch membrane diafiltration processes, and then to operate them optimally both in theory and in experiments.

The modeling is followed by the simulation and implementation of optimal operation. Implementation involves performing the optimal operation on a laboratory scale membrane separation plant via controlling the addition rate of solvent (diluant) into the feed tank in order to reach the final concentrations whilst minimizing costs.

The objectives to be minimized are processing time, or diluant consumption, or both for batch open-loop diafiltration processes. Pontryagin's minimum principle is utilized to attain the analytical solution for optimal operation. The optimal operation derivation is verified experimentally on a plant using nanofiltration form of membrane separation. Case studies are implemented showing the optimal operation and its comparison with the current or traditional industrial strategies of membrane separation.

In case of batch closed-loop diafiltration processes the objectives to be minimized are time, or diluant consumption, or power, or a combination of them. The numerical methods of orthogonal collocations, and control vector parameterization are applied to obtain the optimal operation strategies. Case studies are studied in simulation. The inferences are established regarding the advantages and disadvantages of batch closed-loop over open-loop configuration.

Keywords: Membrane separation, Modeling, Optimal operation, Nanofiltration, Diafiltration, Pontryagin's minimum principle, Batch implementation.

Abstrakt

Cieľom tejto dizertačnej práce je návrh optimálneho riadenia membránových procesov a jeho overenie v laboratórnych podmienkach.

Prvá časť tejto práce sa venuje modelovaniu membránových procesov. Súčasťou je modelovanie rozličných konfigurácií membránových procesov s následným odvodením nových modelov. Taktiež študujeme vlastnosti diafiltračných konfigurácií so zatvoreným (closed-loop) a otvoreným obehom (open-loop) v dávkovom režime.

Modelovanie je nasledované simulácou a implementáciou optimálneho riadenia. Implementácia zahŕňa vykonanie optimálnych operácií riadenia v laboratórnych podmienkach na zariadení vykonávajúcom membránovú filtráciu. Cieľom optimalizácie je analyticky nájsť mieru pridávania rozpúšťadla do vstupnej nádrže za cielom dosiahnutia finálnej koncentrácie pri čo najmenších prevádzkových nákladoch.

Cieľom je minimalizovať procesný čas, rozpúšťadlo, alebo kombináciu týchto veličín pre diafiltračné procesy s otvoreným obehom pre spracovanie v dávkach. Využívame Pontrjaginov princíp minima za účelom dosiahnutia analytického riešenia pre optimálne riadenie. Výsledné odvodené optimálne riadenie je následne overené experimentom na zariadení s použitím nanofiltračnej formy membránovej filtrácie. Prípadové štúdie sú implementované, ukazujúc optimálne riadenie a jeho porovnanie so súčasnými a tradičnými priemyselnými postupmi membránovej filtrácie.

V prípade vsádzkovej diafiltrácie so zatvoreným obehom je cieľom minimalizovať čas spracovania, spotrebu rozpúšťadla, výkonu alebo kombinácie týchto veličín. Použitím numerických metód ortogonálnej kolokácie a parametrizácie vektora riadenia získavame optimálne prevádzkové stratégie. Taktiež študujeme simulačné prípadové štúdie. Zistenia sú zhodnotené na záver v porovnaní výhod a nevýhod konfigurácií so zatvoreným a otvoreným obehom pre vsádzkové procesy.

Kľúčové slová: Membránová separácia, modelovanie, optimálne riadenie, nanofiltrácia, diafiltrácia, Pontrjaginov princíp minima, vsádzkové procesy.

1 Introduction

Products that we require in our modern lives usually exist or are manufactured in combination with other products or unwanted impurities. The objective of separation is to get these product/s purified from these impurities or byproducts. In current era, most of the manual actions and works have been replaced by machines. It applies to the separation process too. Separation is done industrially at a large scale now. Chemical, petrochemical, food, biotechnology, and agriculture industries use separation techniques intensively. The other use of separation in most industries is to clean the effluent water for reuse. The separation can be achieved using techniques like solvent based extraction, distillation, supercritical fluid extraction, sedimentation aided with coagulants and flocculants, etc. The other technique that is widely admired, accepted, and used in industries for separation is membrane filtration.

Membrane process is the separation of two or more different molecules from a solution, or from each other in a solution, using semi-permeable membranes, as described in Cheryan (1998) and Zeman (1996). These membranes are specific filters, designed in order to pass certain molecules, and retain others, based on their size, charge, and ionic properties. Membranes have found numerous applications in water purification (Mallevialle et al., 1996), desalination, TOC (total organic carbon) minimization, juice clarification, product separation and purification (Crespo et al., 1994). The various driving forces for separation in membrane processes are concentration gradient, pressure, and electric potential. The governing principle of separation is based on the molecular size differences of the solutes which pass through the perm-selective membrane with different rates. The process is usually designed to increase the concentration of the valuable product/s, and to decrease the concentration of impurities.

The following points provide the advantages of membrane aided separation over other techniques.

1. Compared to distillation, membrane processes do not require high temperatures for separation. Hence, they prevent denaturation of valuable

bio-products, like anti-bodies, vitamins, and other heat-labile products.

2. The solvent based extraction of product/s adds up the cost of solvent, compared to membrane filtration. It also requires an additional step to remove this used solvent from the extracted product.

3. Membrane based processes do not require chemicals (coagulants, flocculants) for separation. It is much faster and gives higher product purity when compared to these chemical counterparts.

Besides industrialization, automation and control are the other operational requirements that must be dealt with. The first priority is to operate in a way that the required range of product purity is obtained. The next operational priority is to minimize the production/processing/separation costs to accomplish the first priority. Hence, modeling, control, and optimization is performed to achieve the required concentration of product/s, with assurance of cost minimization and minimum manual efforts. There are various methods in theory to design the control strategy to achieve these objectives of product quality and costs. This thesis uses the process knowledge (model, constraints) based derivation of optimal control strategy (both analytical and numerical).

Validation follows the designing of automation and control strategy. We present the results of both, i.e. simulation based and experimental validation.

Diafiltration (DF) is a technique where membrane separation is combined with external addition of a diluant (e.g. pure water), to reduce impurities.. Two diafiltration (DF) membrane separation types are considered:

1. batch diafiltration (batch open-loop DF),

2. batch diafiltration with partial recirculation (batch closed-loop DF).

These processes are considered operating under constant trans-membrane pressure (TMP) and temperature.

The optimal operation of batch DF process is achieved by controlling the addition of diluant into the system in order to attain the desired separation and final required concentrations, whilst minimizing processing costs.

The batch open-loop DF optimization problem is a non-linear dynamic optimization problem. As it is a control-affine problem, Pontryagin's minimum principle (Pontryagin et al., 1962) will be utilized to obtain the optimal operation strategies analytically. In literature, several case studies are solved analytically and numerically in Paulen and Fikar (2016) to optimally operate membrane separation process using diluant rate as the input. The existing models of separation are used in this book (Paulen and Fikar, 2016) from literature. The study is completely in simulation and presents no experimental results. In this thesis batch open-loop DF will be studied in laboratory conditions, and the separation rate will be dynamically modeled based on experimental data (Sharma et al., 2017a, 2018). Further, this experimental model will be used to find the optimal strategy to minimize the processing time, or diluant consumption, or a weighted combination of both. The optimal strategies will be firstly shown in simulation. After simulation, selected case studies will be implemented on a membrane separation plant, and verified experimentally. The traditional industrial strategy will also be performed on the plant to achieve the same objectives, and to compare with the implemented optimal strategies.

In case of batch closed-loop DF there are two manipulated variables: diluant addition rate and recirculation ratio. This process can aim at operation with the objective to minimize time, or to minimize the power required to achieve the separation, or to minimize the diluant addition or multi-objective. This is again a non-linear dynamic optimization problem, but is found to be not affine w.r.t. control inputs. Hence, only theoretical and simulation studies will be presented for this process in thesis.

Thesis Contributions

The main contributions of this thesis can be summarized as follows:

- Study of batch closed-loop DF processes: mathematical modeling, numerical optimization, and case studies together with comparison to batch open-loop DF (Sharma et al., 2015, 2017b).

- Implementation and verification of optimal operation strategy in laboratory conditions for batch open-loop DF processes, comparison of the proposed optimal strategies with the traditional ones (Sharma et al., 2018, 2019).

Some partial results were obtained for parameter estimation problems for open-loop diafiltration using experimental data (Sharma et al., 2016a, 2017a, 2018).

Additionally, I also contributed as a team member to results in optimal control of membrane processes subject to fouling (Jelemenský, 2016; Jelemenský et al., 2015a,b, 2016).

2 Diafiltration Process

Diafiltration can be used for separation of two or more solutes from one another (e.g. separation of a salt/s from protein/s or sugar/s or both, separation of sugar/s from protein/s, or indeed separation of one protein/sugar from another protein/sugar), and especially for reducing the concentration of micro-solute (impurity), by the addition of a diluant. Hence, it can be used for concentrating product or reducing impurity, or both. The membrane used should allow easy passage of the solute desired in the permeate while substantially retaining the other solute.

The batch membrane diafiltration plant studied in this thesis consists of the following crucial parts:

- feed tank – it is the source for the feed solution, and as it is a batch process no feed is added during the run,
- feed pump (P1) – it is the pump that forces the solution from feed tank towards the membrane,
- membrane (M) – it is the source for the separation of solutes (product and impurity),
- diluant pump (P3) – it is needed to force the diluant into the tank at controlled rate.

2.1 Diafiltration – Open-loop Configuration

As shown in Fig 1(a), the feed pump pushes the feed towards the membrane at desired pressure. Through the membrane the feed gets separated in two streams: retentate stream, i.e. the concentrated stream with macro-solute/s, which returns back to the feed tank, and the permeate stream comprising of micro-solute/s or just solvent, that leaves the system. In this configuration, the retentate is completely recycled back to the feed tank and hence it is also known as open loop batch (Fig 1(a)). A batch concentration process is usually operated at constant transmembrane pressure. Due to the continuous increase of solute concentration in the feed, the permeate flux declines with time.

2.2 Diafiltration with Partial Recirculation Plant – Closed-loop Configuration

As in batch plant, this configuration too has a feed tank, a semi-permeable membrane, and a feed pump. Besides these, closed-loop configuration additionally has a recirculation loop, and a recirculation pump (Fig. 1(b)).

In this configuration, the feed goes to the membrane from tank and the retentate returns back to the tank but some portion of the retentate flow can be directed back through a recirculation pipe (Fig. 1(b)) and pump to the membrane. The retentate splitting ratio could range between 0 and 1. This system or membrane operation according to Todaro and Vogel (2014), Mallevialle et al. (1996), is also called *Batch closed loop* operation. Closed loop batch or topped-off batch as mentioned in Cheryan (1998) is used when permeate is the required product, for e.g., fruit juice clarification and microfiltration of whey. The batch closed-loop operation has following advantages over traditional batch (open-loop) operating mode:

1. This configuration provides a controlled and defined flow rate, irrespective of the degree of fouling and changes in feed composition (Rapaport, 2006).

2. The pipe diameter can be smaller than in conventional batch (Cheryan, 1998; Rapaport, 2006).

3. The feed tank size can also be smaller for the closed-loop setup as part of the solution volume is permanently inside the loop. This reduces problems of foaming Cheryan (1998); Tamime (2012). Temperature and quality of sensitive retentate products can be maintained which can be difficult in open-loop batch (AWWA, 2005).

4. For large systems with remote tankage this setup can save quite a lot of large piping and with a small pressurizing feed pump, a large amount of energy by keeping the loop pressure high (Dow Water & Process Solutions; Jornitz and Meltzer, 2007; Rapaport, 2006).

5. In membrane bioreactors, partial recycle of retentate resulted in higher

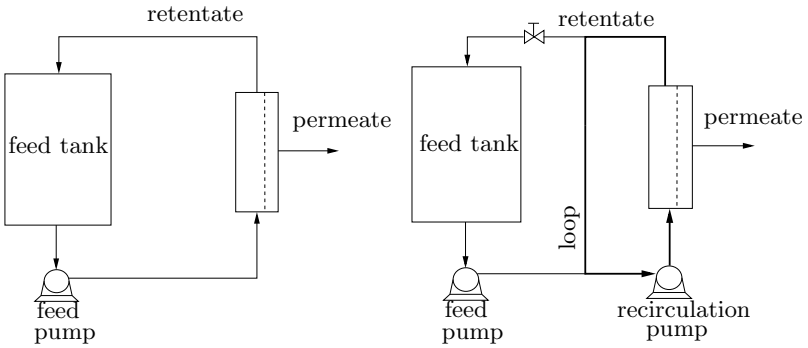

(a) Complete recycle of retentate (b) Partial recycle of retentate

Figure 1: Batch membrane diafiltration with complete (open-loop) and partial recirculation (closed-loop) of retentate.

nutrient uptake, which helped producing a higher biomass concentration (Bilad et al., 2014).

3 Optimal Control – Open-Loop Batch Diafiltration

3.1 Process Model

The mathematical model of batch open-loop diafiltration membrane processes is presented here. This model has been adapted from literature (Kovács et al., 2009).

Two component/solute solution has been used for all experimental batch open-loop work. The solutes used are lactose (c_1) and NaCl (c_2). The experiments in this thesis are for concentrating lactose and reducing NaCl's concentration, using nanofiltration (NF) based diafiltration (NDF). The NDF model for the two component solution can be described by the following three

differential equations

$$\frac{\mathrm{d}c_1}{\mathrm{d}t} = \frac{c_1 q_\mathrm{p}}{V}(R_1 - \alpha), \qquad c_1(0) = c_{1,0}, \tag{1a}$$

$$\frac{\mathrm{d}c_2}{\mathrm{d}t} = \frac{c_2 q_\mathrm{p}}{V}(R_2 - \alpha), \qquad c_2(0) = c_{2,0}, \tag{1b}$$

$$\frac{\mathrm{d}V}{\mathrm{d}t} = (\alpha - 1)q_\mathrm{p}, \qquad V(0) = V_0, \tag{1c}$$

where the constants R_1, R_2 are rejection coefficients of lactose and NaCl respectively.

It was observed during our preliminary experiments that the rejections for both lactose and NaCl stay around constant values. $R_i = 0$ implies that the ith solute passes through the membrane without any resistance. This is the case for the used membrane as it does not resist to a free passage of NaCl, hence $R_2 = 0$. On the contrary, $R_i = 1$ means that the membrane blocks the solute completely and its concentration in the permeate is zero, which is the property of membrane regarding rejection of lactose. Because of $R_1 = 1$ (at any time, mass of lactose stays constant),

$$c_1 V = c_{1,0} V_0 \quad \Rightarrow \quad c_1 = \frac{c_{1,0} V_0}{V}. \tag{2}$$

Eq. (2) can be used to eliminate volume from the model (1). This transforms the general model from three to two differential equations, i.e.

$$\frac{\mathrm{d}c_1}{\mathrm{d}t} = c_1^2 \frac{q_\mathrm{p}}{c_{1,0} V_0}(1 - \alpha), \qquad c_1(0) = c_{1,0}, \tag{3a}$$

$$\frac{\mathrm{d}c_2}{\mathrm{d}t} = -c_1 c_2 \frac{q_\mathrm{p}}{c_{1,0} V_0}\alpha, \qquad c_2(0) = c_{2,0}. \tag{3b}$$

3.1.1 Diluant Input Modes

The dilution rate or input ($\alpha \geq 0$) as discussed, is the dynamic degree of freedom for the NDF process. The classical operation of batch NDF or DF mostly uses piece-wise constant α using three simple modes (Foley, 2006; Jaffrin and Charrier, 1994):

- No diluant input ($\alpha = 0$), i.e. concentration mode (C): in this mode, the volume decreases (1c), and the mass of lactose is constant. As a result,

the concentration of lactose increases (1a), while the concentration of NaCl stays constant (1b).

- The diluant inflow equals the outflow of permeate ($\alpha = 1$), i.e. constant volume diafiltration mode (CVD): lactose concentration remains constant (1a), as does the volume (1c), while NaCl concentration decreases in this mode due to dilution done by adding pure water as diluant (1b).

- Diluant flow-rate is less than the outflow of permeate ($0 < \alpha < 1$), i.e. variable volume diafiltration mode (VVD): volume decreases in this mode (1c), and hence lactose concentration increases (1a), while due to the dilution of solution, NaCl concentration decreases as well (1b).

In addition to these three modes, Lutz (2015); Paulen and Fikar (2016) have proposed two new basic modes:

- Dynamic volume diafiltration (DVD): this is similar to VVD mode as diluant flow-rate is less than the outflow of permeate, but unlike VVD α is not a constant but is varying with time ($0 < \alpha(t) < 1$).

- Pure dilution mode (D): in this mode a certain amount of diluant is instantaneously added to the solution. This can be represented by $\alpha = \infty$. Lactose and NaCl concentrations decrease proportionally in pure dilution mode. Due to the nature of this step, it can be done without the plant/process running (no energy used), and takes negligible amount of time.

Combination of different modes results in different costs and time to achieve certain concentration of product and impurities (Paulen et al., 2013).

3.2 Laboratory Membrane Plant

This section describes the batch open-loop DF plant utilized to achieve these experimental objectives Fig. 2. The plant has also been used in education process (Sharma et al., 2016b). NFW-1812F nanofilter membrane manufactured by Synder Filtration, USA, with a cut-off range 300–500 Da, and a membrane area of $A = 0.465\,\mathrm{m}^2$ was used to perform the experiments.

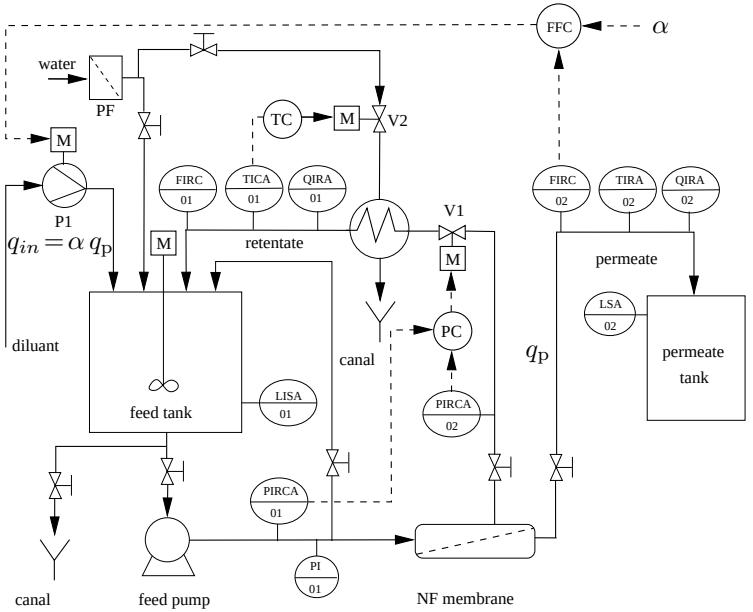

Figure 2: P&I diagram of the laboratory nanodiafiltration process.

The following steps describe the procedure of experiments.

1. The initial feed volume is added to the feed tank comprising the initial concentrations of lactose ($c_{1,0}$) and NaCl ($c_{2,0}$).

2. At a fixed pumping power, resulting in certain pressure, the feed is pushed towards the membrane in cross-flow mode. The operation is started in the total recirculation mode, i.e. both the permeate and the retentate return to the feed tank. The concentrations and volume hence stay constant. This is done to stabilize:

    - The transmembrane pressure (TMP = (PIRCA01 + PIRCA02)/2 - atmospheric pressure), where sensor PIRCA01 measures membrane inlet, while PIRCA02 measures retentate pressure,
    - The temperature of the solution,
    - The hydrodynamic conditions, and to eliminate the initial fouling (Sharma et al., 2016a, 2017a).

After this stabilization, the experiment is started by letting the permeate leave the system towards the permeate tank.

HMI designed using WinCC environment, and Simulink based HMI are used for the data visualization, storage, etc.

The permeate flow-rate is measured using sensor FT02 (see Fig. 2). The concentration of NaCl ($c_2\,[\mathrm{kg/m^3}]$) in the retentate is inferred from the conductivity measurements (sensor QT01) . The calibration curve obtained is represented by using the experimentally obtained linear model

$$c_2 = 0.0007 \times \mathrm{QT}\,[\mu\mathrm{S/cm}] - 0.6949, \tag{4}$$

where QT represents the actual retentate conductivity.

The experiments done for the solution of lactose and NaCl (Sharma et al., 2016a, 2017a, 2018) show that the retentate comprises lactose and NaCl, while the permeate contains NaCl only.

Lactose concentration ($c_1\,[\mathrm{kg\,m^{-3}}]$) at each sampling instance is calculated from the known initial mass, and the actual volume/level in the feed tank (LISA01). This is due the properties of the used membrane (Synder, 2014), that retains lactose in the system. Hence, the mass of lactose in the system, at any time during the experiment stays constant. Consequently, the concentration of lactose at any time is given by (2). Controllers were designed and implemented to regulate temperature (TC), pressure (PC) and the diluant input rate (FFC).

3.3 Experimental Modeling

The permeate flow rate (q_p) present in the model equations is generally a function of concentration, pressure and temperature for a given membrane. In this thesis, constant pressure and temperature are maintained. Therefore, the permeate flow rate is only a function of concentrations. This relation needs to be identified and parameterized experimentally in order to develop the further research on this process. This experimental modeling work has been published in Sharma et al. (2016a, 2017a, 2018).

Two different models were fitted with the permeate flow rate data

Table 1: Parameters of the models.

model	GLF	LF_1	LF_2
γ_1	3.0	2.8	3.4
γ_2	1109.9	1246.7	723.7
γ_3	0.1	-	-

- Limiting flux (LF) model: This model has been taken from Balannec et al. (2005); Blatt et al. (1970); Tang and Leckie (2007). The model defines the permeate flow rate as a function of time-varying lactose (macro-solute) concentration and the parameters, i.e. mass transfer coefficient ($\gamma_1\,\mathrm{mh}^{-1}$) and limiting concentration of lactose ($\gamma_2\,\mathrm{mh}^{-1}$).

$$q_\mathrm{p} = k\,A \ln\left(\frac{c_\mathrm{lim}}{c_1}\right) = A\left(\gamma_1 + \gamma_2 \ln(c_1)\right), \tag{5}$$

  Two variation of this model were fitted. Firstly, by taking the complete experimental data including C and CVD modes, i.e. LF_1. Secondly, using only the data from the first part of experiment (C mode), i.e. LF_2.

- Generalized limiting flux (GLF) model: Based on the preliminary experiments, a form of the model of q_p used in this work is defined as generalized limiting flux model (GLF), (Rajagopalan and Cheryan, 1991)

$$q_\mathrm{p} = A\left(\gamma_1 + \gamma_2 \ln(c_1) + \gamma_3 \ln(c_2)\right), \tag{6}$$

  It incorporates concentrations of both solutes and can be reduced to the limiting flux model with $\gamma_3\,\mathrm{mh}^{-1} = 0$.

The resulting model parameters are given in the Table 1.

3.4 Optimal Control

The objective of the membrane process optimization is to find a time-dependent input function $\alpha(t)$, that drives lactose and NaCl concentration from initial value $[c_{1,0},\, c_{2,0}]$ to final value $[c_{1,\mathrm{f}},\, c_{2,\mathrm{f}}]$, whilst minimizing the operating costs.

3.4.1 Problem Formulation

The operating costs can be minimized in various ways. The most common is minimization of the processing time

$$t_{\mathrm{f}}^{*} = \min_{\alpha(t)} t_{\mathrm{f}} = \min_{\alpha(t)} \int_{0}^{t_{\mathrm{f}}} 1 \, \mathrm{d}t, \tag{7}$$

where t_{f} denotes the time needed to bring the process from the given initial concentrations to desired final ones. Another generally used cost function is the total volume of diluant used to reach the desired concentrations i.e.

$$V_{\mathrm{D}}^{*} = \min_{\alpha(t)} V_{\mathrm{D}} = \min_{\alpha(t)} \int_{0}^{t_{\mathrm{f}}} q_0 \, \mathrm{d}t = \min_{\alpha(t)} \int_{0}^{t_{\mathrm{f}}} \alpha q_{\mathrm{p}} \, \mathrm{d}t. \tag{8}$$

In order to incorporate both processing time (t_{f}) and diluant consumption (V_{D}), a weighted objective function can be defined i.e.

$$\mathcal{J}^{*} = \min_{\alpha} \; w_{\mathrm{T}} t_{\mathrm{f}} + w_{\mathrm{D}} V_{\mathrm{D}}, \tag{9a}$$

s.t.

$$\dot{c}_1 = c_1^2 \frac{q_{\mathrm{p}}}{c_{1,0} V_0} (R_1 - \alpha), \qquad c_1(0) = c_{1,0}, \tag{9b}$$

$$\dot{c}_2 = c_1 c_2 \frac{q_{\mathrm{p}}}{c_{1,0} V_0} (R_2 - \alpha), \qquad c_2(0) = c_{2,0}, \tag{9c}$$

$$c_1(t_{\mathrm{f}}) = c_{1,\mathrm{f}}, \quad c_2(t_{\mathrm{f}}) = c_{2,\mathrm{f}}, \tag{9d}$$

$$q_{\mathrm{p}} = q_{\mathrm{p}}(c_1, c_2). \tag{9e}$$

The non-negative weighting coefficients $w_{\mathrm{T}}, w_{\mathrm{D}}$ represent the weight (or price) for a unit of processing time and diluant consumption, respectively.

3.4.2 Problem Solution

As per Paulen and Fikar (2016) and Pontryagin's minimum principle (Pontryagin et al., 1962). The optimal diluant addition strategy consists of three successive operation modes, where the first and the last mode corresponds to operation with α being saturated on constraints (either C or pure dilution mode). The second mode is characterized by the singular curve equation ($S = 0$) and diluant rate α, being function of both solute's concentra-

tions (Paulen and Fikar, 2016)

$$S = w_{\mathrm{T}}\left(q_{\mathrm{p}} + \frac{\partial q_{\mathrm{p}}}{\partial c_1}c_1 + \frac{\partial q_{\mathrm{p}}}{\partial c_2}c_2\right) + w_{\mathrm{D}}q_{\mathrm{p}}^2 = 0, \tag{10}$$

$$\alpha = \frac{\frac{\partial S}{\partial c_1}c_1}{\frac{\partial S}{\partial c_1}c_1 + \frac{\partial S}{\partial c_2}c_2}. \tag{11}$$

The middle mode for the lactose-salt system for the GLF model (6), using singular curve (10) and singular control equation (11) is given as

$$\begin{aligned} S(c_1, c_2) = A\, w_{\mathrm{T}}(\gamma_1 + \gamma_2 + \gamma_3 + \gamma_2 \ln c_1 + \gamma_3 \ln c_2) \\ + A^2\, w_{\mathrm{D}}(\gamma_1 + \gamma_2 \ln(c_1) + \gamma_3 \ln(c_2))^2 = 0, \end{aligned} \tag{12}$$

$$\alpha = \frac{\gamma_2}{\gamma_2 + \gamma_3} = 0.914. \tag{13}$$

Hence, the optimal middle mode for this system with GLF model is VVD. The optimal concentration of macro-solute (lactose) to switch to the middle mode can be derived from (12) for the following three cases:

1. Multi-objective i.e. $w_{\mathrm{T}} > 0$ and $w_{\mathrm{D}} > 0$:

$$c_1^* = \exp\left(-\frac{\gamma_1 + \gamma_3\, \ln(c_2) + \frac{w_{\mathrm{T}} - \sqrt{w_{\mathrm{T}}}\sqrt{(w_{\mathrm{T}} + (\gamma_2 - \gamma_3)4Aw_{\mathrm{D}})}}{2Aw_{\mathrm{D}}}}{\gamma_2}\right), \tag{14}$$

2. Time-optimal i.e. $w_{\mathrm{T}} > 0$ and $w_{\mathrm{D}} = 0$:

$$c_1^* = \exp\left(-\frac{\gamma_1 + \gamma_2 + \gamma_3 + \gamma_3\, \ln(c_2)}{\gamma_2}\right), \tag{15}$$

3. Diluant-optimal i.e. $w_{\mathrm{T}} = 0$ and $w_{\mathrm{D}} > 0$:

$$c_1^* = \exp\left(-\frac{\gamma_1 + \gamma_3\, \ln(c_2)}{\gamma_2}\right). \tag{16}$$

The first and the third mode are either C ($\alpha = 0$) or D ($\alpha = \infty$) mode. This depends on initial and desired final concentrations w.r.t. to the singular curve (the sign of $S(c_{1,0}, c_{2,0})$ and $S(c_{1,\mathrm{f}}, c_{2,\mathrm{f}})$). In the first section one takes the mode that brings the concentrations of the solutes to the singular curve ($S(c_1, c_2) = 0$ or c_1^*). Hence, if the initial concentration of macro-solute is less than optimal switching concentration, then we need to use C mode to increase

macro-solute's concentration to reach there. On the contrary, we need to reduce macro-solute's concentration using D mode if initial concentration of macro-solute is more than optimal switching concentration. These cases for initial mode are:

$$\alpha = \begin{cases} 0\,(\text{C mode}), & \text{if } c_{1,0} < c_1^*, \\ \infty\,(\text{D mode}), & \text{if } c_{1,0} > c_1^*, \text{ and} \\ \alpha_s, & \text{if } c_{1,0} = c_1^*. \end{cases} \tag{17}$$

The third section starts at singular curve and chooses the mode that finishes at the desired final concentrations. That is, if the macro-solute is over-concentrated than its final concentration at the end of second (singular) section, then D mode needs to be applied to dilute the solution and reach the final concentrations. On the contrary, if the macro-solute was not concentrated enough during the previous two modes, C mode needs to be applied again to reach the final concentrations.

Now, for the limiting flux model (5), using the same general singular curve (10) and singular control equation (11), the optimal switching condition and control can be given as

$$\begin{aligned} S(c_1, c_2) = w_{\mathrm{T}}\, A\, k \Big(\ln \frac{c_{\lim}}{c_1} - 1 \Big) \\ + w_{\mathrm{D}}\, A^2\, k^2 \ln \Big(\frac{c_{\lim}}{c_1} \Big)^2 = 0, \end{aligned} \tag{18}$$

$$\alpha = \frac{\frac{\partial S}{\partial c_1} c_1}{\frac{\partial S}{\partial c_1} c_1} = 1. \tag{19}$$

Therefore, the optimal middle control in case of limiting flux is CVD. Note: the optimality of CVD in minimum-time (time-optimal) case was previously found by Ng et al. (1976).

For limiting flux model, the optimal switching concentration of lactose to the middle mode can be found analytically for;

1. Multi-objective i.e. $w_{\mathrm{T}} > 0$ and $w_{\mathrm{D}} > 0$:

$$c_1 = c_{\lim} \exp \left(\frac{w_{\mathrm{T}} - \sqrt{w_{\mathrm{T}}^2 + 4kAw_{\mathrm{T}}w_{\mathrm{D}}}}{2Akw_{\mathrm{D}}} \right), \tag{20}$$

2. Time-optimal i.e. $w_{\mathrm{T}} > 0$ and $w_{\mathrm{D}} = 0$:

$$c_1 = \frac{c_{\mathrm{lim}}}{\mathrm{e}}, \tag{21}$$

3. Diluant-optimal i.e. $w_{\mathrm{T}} = 0$ and $w_{\mathrm{D}} > 0$:

$$c_1 = c_{\mathrm{lim}}. \tag{22}$$

The modes to be applied in first and third section depend on the initial and final conditions w.r.t. the singular curve.

The middle optimal control for both models is constant, but different. The singular curve is also different for the models, and this translates into changes in start and end points (concentrations) of the middle mode.

3.5 Optimal Control – Case Studies

The case studies serve to demonstrate both in simulations and experiments, the proposed optimal membrane separation strategy (section 3.4) using batch open-loop NDF, and its advantages to existing (traditional) industrial strategies (published in Sharma et al. (2019) and Sharma et al. (2018)). Lactose monohydrate (M = 360.31 g/mol) is the purified and concentrated product while sodium chloride (M = 58.44 g/mol) is the impurity to be removed. Reverse osmosis water is used as a solvent to prepare solutions, and also as the diluant for DF. The results of optimal scenarios in these case studies are based on the GLF permeate flow model parameterized in the previous section.

For the two case studies presented here out of the three cases studies from the thesis, the process initial conditions are as follows: the volume of the solution $V_0 = 0.032\,\mathrm{m}^3$, the lactose concentration $c_{1,0} = 48\,\mathrm{kg/m}^3$ and the salt concentration $c_{2,0} = 6\,\mathrm{kg/m}^3$. The difference in case study 1 and 2 lies in the final concentrations. We will study two possible final concentration sets:$(c_{1,\mathrm{f}}, c_{2,\mathrm{f}}) = (155\,\mathrm{kg/m}^3, 1\,\mathrm{kg/m}^3)$ and $(c_{1,\mathrm{f}}, c_{2,\mathrm{f}}) = (470\,\mathrm{kg/m}^3, 3\,\mathrm{kg/m}^3)$. These initial and final points are shown in Fig. 3 together with the singular curve (12) for minimum time settings ($w_{\mathrm{D}} = 0$). The final points are chosen so that they are positioned to the left and to the right of the singular curve, respectively.

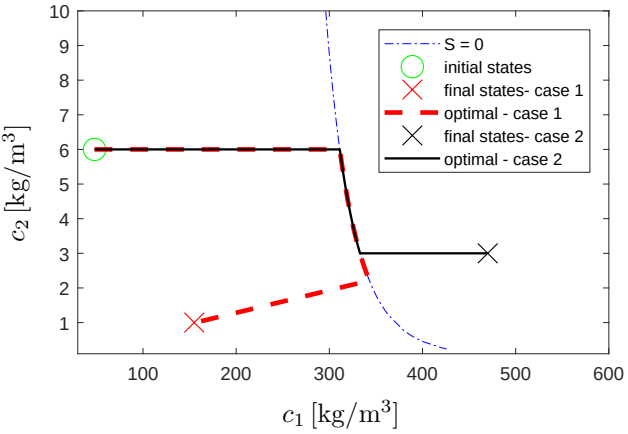

Figure 3: Concentration diagram for case studies along with the singular curve ($S = 0$).

As the initial point is located to the left of the singular curve, the optimal initial operation mode for both cases is the C mode. When the final point lies to the left of the singular curve, the optimal terminal (third) operation mode is the D mode. In the opposite case another C mode is used to finish the processing.

3.5.1 Case Study 1

Three strategies were experimentally tested:

Traditional two step strategy C-CVD: ($\alpha = \{0, 1\}$): pure NF using the C mode until lactose concentration increases to the desired final value ($c_1 = c_{1,\mathrm{f}} = 155\,\mathrm{kg/m^3}$) followed by the CVD mode to reduce NaCl concentration to the final value ($c_2 = c_{2,\mathrm{f}} = 1\,\mathrm{kg/m^3}$).

Time-optimal strategy C-VVD-D: ($\alpha = \{0, 0.914, \infty\}$), $w_\mathrm{D} = 0$: The concentration mode is used to keep the salt concentration constant $c_2 = c_{2,0} = 6\,\mathrm{kg/m^3}$ and to increase the lactose concentration to $c_1 = \exp\big(-(\gamma_1 + \gamma_2 + \gamma_3 + \gamma_3 \ln c_2)/\gamma_2\big) = 311.2\,\mathrm{kg/m^3}$, which follows from (12). Then, the VVD mode is applied until the condition $c_1/c_2 = c_{1,\mathrm{f}}/c_{2,\mathrm{f}}$ is met. This ends the separation process and an ap-

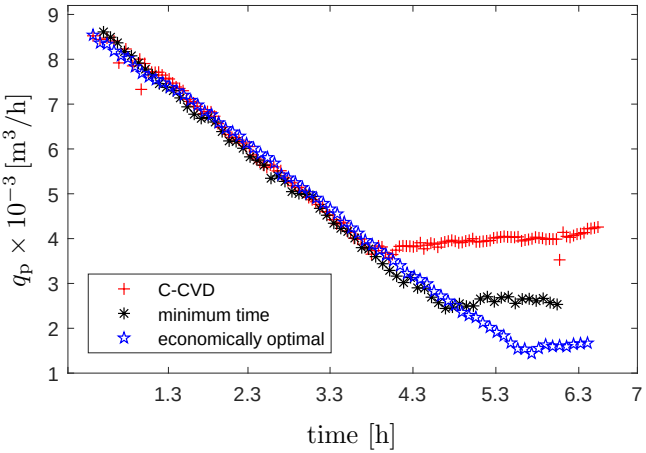

Figure 4: Case study 1: Permeate flow-rate measurements of traditional and optimal strategies.

propriate amount of water is added to the solution.

Economically optimal strategy C-VVD-D: ($\alpha = \{0, 0.914, \infty\}$), $w_T = 1 €/h, w_D = 0.2 €/m^3$. The only difference to the time-optimal strategy is the lactose concentration to be reached in the concentration mode. The singular curve (12) is shifted to the right in the concentration diagram and the VVD mode is applied when $c_1 = 438.2\,kg/m^3$. This switching concentration is found numerically using the values of w_T, w_D from (12).

The switching concentration of lactose is quite high in both of the optimal cases. The solubility of lactose at the given temperature is lower than that of our requirements (Yalkowsky et al., 2016). However, as lactose is totally retained by the membrane, so it does not effect significantly our optimal strategy and the process of separation. Moreover, due to high flow rate of retentate returning to the tank, the solution was continuously mixed/stirred, and lactose was not observed to be settled at the bottom or segregated in pipes. Hence, the only significant variable effected by lactose concentration is q_p, and that we have studied and modeled in this thesis.

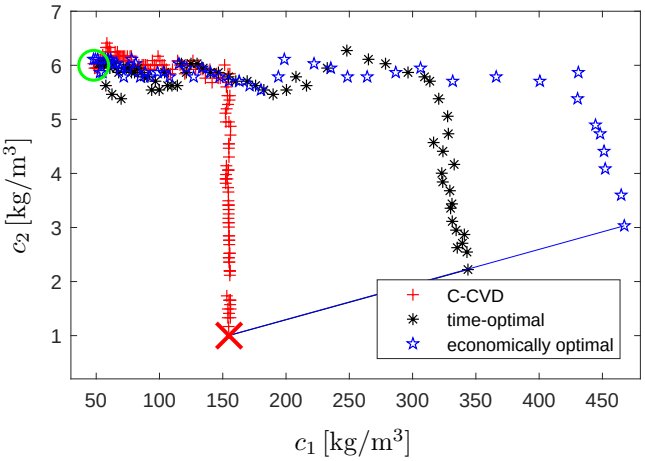

Figure 5: Case study 1: Concentration measurements of lactose and NaCl for traditional and optimal strategies.

Measurements from the conducted experiments are presented in the permeate flow-rate diagram (Fig. 4) and in the concentration diagram (Fig. 5). The permeate diagram shows that although the duration of the concentration mode is the shortest in the classical strategy, the subsequent CVD mode makes the final processing time the longest.

The concentration diagram (Fig. 5) shows initial and final points (green and red circles, respectively) as well as solid lines indicating dilution mode at the end of processing with optimal strategies.

Table 2 summarizes experimentally obtained values of final processing times and water consumption. Relative values $\Delta t_\mathrm{f}, \Delta V_\mathrm{D}$ take the maximum value in the column as 100% and show reduction in other experiments (e.g. time-optimal takes only 92.5% of time required by C-CVD approach). The cost in the table is calculated by taking the price per unit of time and diluant volume from the economically optimal strategy ($w_\mathrm{T} = 1\,€/\mathrm{h}, w_\mathrm{D} = 0.2\,€/\mathrm{m}^3$).

We can notice that the traditional strategy is worse in both the indicators compared to the proposed optimal ones. These take 92-98 % of the processing time and 74-86 % of the diluant consumption. Although the economically optimal strategy is close to the traditional one in the terms of the processing

Table 2: Experimental results: comparison of total processing time and diluant consumption for different scenarios in case study 1.

Strategy	t_f [h]	Δt_f [%]	$V_D \times 10^{-3}$ [m^3]	ΔV_D [%]	Cost [€]
traditional (C-CVD)	6.53	100.00	10.69	100.00	6.53
time-optimal	6.04	92.50	9.16	85.61	6.04
economically optimal	6.40	98.01	7.96	74.39	6.40

times, its diluant usage is significantly lower.

It is worth noting that besides reducing processing time and diluant consumption, the optimal strategies can be applied with existing setup comparable to the industrial standard and without any new hardware. Also, no on-line optimization/calculations are required: the switching concentrations and control is found out prior to the start of an experiment.

Further improvement can be achieved by re-estimating the model parameters while performing the separation (online parameter estimation). This may result in implementation of a truly real-time optimal strategy, but at the expense of online optimization/calculations, and hardware/software modifications.

3.5.2 Case Study 2

Three strategies were implemented and compared:

Traditional two step strategy C-CVD: ($\alpha = \{0, 1\}$): pure NF using the C mode till lactose concentration increases to the desired final value ($c_1 = c_{1,f} = 470\,\mathrm{kg/m^3}$) followed by the CVD mode to reduce NaCl concentration to the final value ($c_2 = c_{2,f} = 3\,\mathrm{kg/m^3}$).

Traditional three step strategy C-CVD-C: ($\alpha = \{0, 1, 0\}$): using the limiting flux model (Ng et al., 1976), apply the concentration mode until lactose concentration increases to ($c_1 = c_{\mathrm{lim}}/\mathrm{e} = 458\,\mathrm{kg/m^3}$) followed by the CVD mode to reduce NaCl concentration to the final value

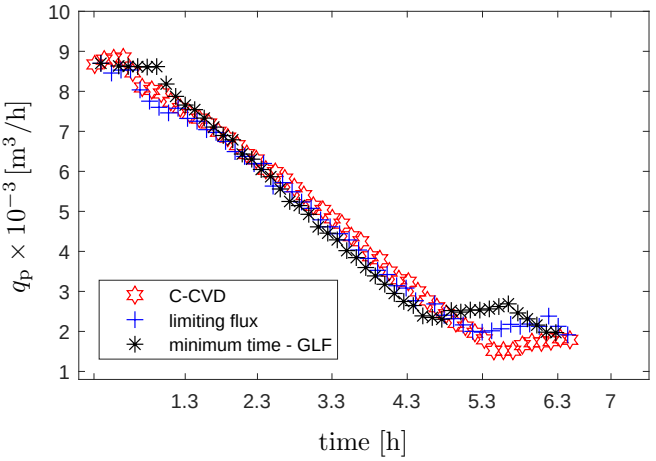

Figure 6: Case study 2: Permeate flow-rate measurements of traditional and optimal strategies.

($c_2 = c_{2,\mathrm{f}} = 3\,\mathrm{kg/m^3}$). The third step is again the C mode to concentrate lactose to its desired final concentration $c_1 = c_{1,\mathrm{f}} = 470\,\mathrm{kg/m^3}$.

Time-optimal strategy C-VVD-C: ($\alpha = \{0, 0.914, 0\}$), $w_\mathrm{D} = 0$: The concentration mode is used to increase the lactose concentration to $c_1 = 311.2\,\mathrm{kg/m^3}$ which follows from (12). Then, the VVD mode is applied until NaCl concentration equals to the final value ($c_2 = c_{2,\mathrm{f}} = 3\,\mathrm{kg/m^3}$). The third step is again the C mode to concentrate lactose to its final concentration $c_1 = c_{1,\mathrm{f}} = 470\,\mathrm{kg/m^3}$.

The experimental results are shown in Figs. 6, 7 and Table 2. The permeate flow-rate diagram, (Fig. 6) shows that all three strategies started at a similar initial flow rate due to the identical initial concentrations. The initial trajectory of flow rate during the C mode is the same for all three of them. The flow-rate trajectory is different in the later part due to difference in inputs for different strategies. The flow-rate in the three step strategies reduces, then stays around a constant value, and finally reduces again. On the other hand, for the C-CVD two step strategy, the flow-rate reduces while concentrating lactose and increases slightly while reducing NaCl. However, only negligible differences can be observed in the final processing times.

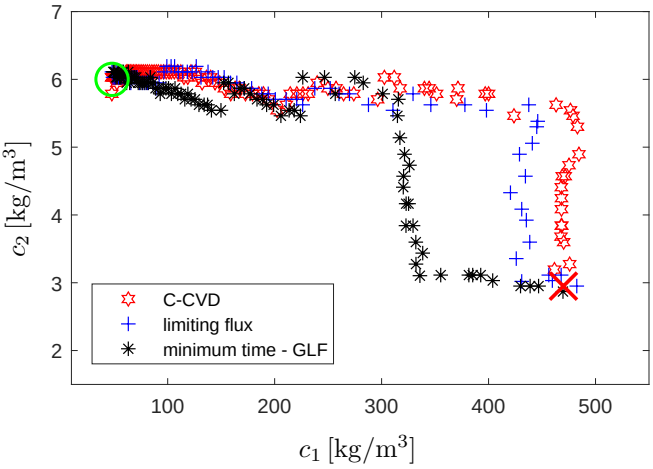

Figure 7: Case study 2: Concentration measurements of lactose and NaCl for traditional and optimal strategies.

When comparing the concentration diagrams, both traditional strategies apply the CVD step at higher lactose concentration whereas the optimal strategy switches to the VVD mode earlier (Fig. 7). The initial and final concentrations are represented by same markers as in case study 1.

Table 3 presents experimental results for processing time and diluant consumption. As also observed from figures, time-optimal strategy does not bring much improvement and there is no reason to abandon classical strategies in this case.

Simulation results for diluant minimization show consumption of only $V_\mathrm{D} = 1.63 \times 10^{-3}\,\mathrm{m}^3$ i.e. 48% of diluant needed by the time optimal strategy. This strategy is C-VVD-D, and takes the longest to get to the final concentrations ($t_\mathrm{f} = 7.2\,\mathrm{h}$). The switching concentration to D mode for this strategy is very high ($917\,\mathrm{kg/m}^3$) and unattainable on this plant.

The case studies experimentally demonstrated and proved that the optimal operation strategies resulted in economic benefits.

Table 3: Experimental comparison of total processing time and diluant consumption for different scenarios in case study 2.

Strategy	t_f [h]	Δt_f [%]	$V_\mathrm{D} \times 10^{-3}$ [m^3]	ΔV_D [%]	Cost [€]
traditional (C-CVD)	6.54	100	2.37	75.72	7.01
limiting flux	6.38	97.75	2.65	84.76	6.91
time-optimal: GLF	6.34	97.00	3.13	100.00	6.97

4 Optimal Control – Batch Closed-Loop Diafiltration

4.1 Process Model

The complete model can then be described by the following system of ordinary differential and algebraic equations:

$$\frac{\mathrm{d}V_\mathrm{T}}{\mathrm{d}t} = (\alpha - 1)q_\mathrm{p}, \qquad V_\mathrm{T}(0) = V_0 - V_\mathrm{L} \tag{23a}$$

$$V_\mathrm{T}\frac{\mathrm{d}c_{\mathrm{T},1}}{\mathrm{d}t} = c_{\mathrm{L},1}s(q_\mathrm{L} - q_\mathrm{p} + q_\mathrm{p}R_1) - c_{\mathrm{T},1}[s(q_\mathrm{L} - q_\mathrm{p}) + \alpha q_\mathrm{p}], \qquad c_{\mathrm{T},1}(0) = c_{1,0}, \tag{23b}$$

$$V_\mathrm{T}\frac{\mathrm{d}c_{\mathrm{T},2}}{\mathrm{d}t} = c_{\mathrm{L},2}s(q_\mathrm{L} - q_\mathrm{p} + q_\mathrm{p}R_2) - c_{\mathrm{T},2}[s(q_\mathrm{L} - q_\mathrm{p}) + \alpha q_\mathrm{p}], \qquad c_{\mathrm{T},2}(0) = c_{2,0}, \tag{23c}$$

$$\begin{aligned} V_\mathrm{L}\frac{\mathrm{d}c_{\mathrm{L},1}}{\mathrm{d}t} &= c_{\mathrm{T},1}[sq_\mathrm{L} + q_\mathrm{p}(1-s)] \\ &\quad + c_{\mathrm{L},1}[-q_\mathrm{L}s - q_\mathrm{p} - q_\mathrm{p}R_1 s + q_\mathrm{p}s + q_\mathrm{p}R_1], \qquad c_{\mathrm{L},1}(0) = c_{1,0}, \end{aligned} \tag{23d}$$

$$\begin{aligned} V_\mathrm{L}\frac{\mathrm{d}c_{\mathrm{L},2}}{\mathrm{d}t} &= c_{\mathrm{T},2}[sq_\mathrm{L} + q_\mathrm{p}(1-s)] \\ &\quad + c_{\mathrm{L},2}[-q_\mathrm{L}s - q_\mathrm{p} - q_\mathrm{p}R_2 s + q_\mathrm{p}s + q_\mathrm{p}R_2], \qquad c_{\mathrm{L},2}(0) = c_{2,0}. \end{aligned} \tag{23e}$$

The total liquid volume is given by an algebraic equation as

$$V = V_{\mathrm{T}} + V_{\mathrm{L}}. \tag{23f}$$

Similarly, the total concentration of a component is influenced by its respective tank and loop concentrations, and can be written as

$$c_i = \frac{V_{\mathrm{T}} c_{\mathrm{T},i} + V_{\mathrm{L}} c_{\mathrm{L},i}}{V_{\mathrm{T}} + V_{\mathrm{L}}} \quad i = 1, 2. \tag{23g}$$

The model (23) thus comprises 5 differential and 3 algebraic equations. The model variables are the tank and total volumes (V_{T}, V), the tank, loop, and total concentrations $(c_{\mathrm{T},1}, c_{\mathrm{T},2},\ c_{\mathrm{L},1}, c_{\mathrm{L},2},\ c_1, c_2)$. There are two degrees of freedom: diluant rate α and recirculation ratio s that serve as manipulated variables.

4.2 Optimal Control

The process optimization of batch closed-loop DF as in batch open-loop DF, can aim at minimizing the processing time (7), and/or diluant consumption (8). In addition, the batch closed-loop configuration has the potential to reduce the power requirements of the separation process. The power minimization problem can be formulated as

$$\mathcal{J}_{\mathrm{P}}^* = \min_{\alpha(t), s(t)} \int_0^{t_{\mathrm{f}}} q_1 \, \mathrm{d}t. \tag{24}$$

4.2.1 Problem Formulation

The multi-objective optimal control problem can then be defined as follows

$$\mathcal{J}^* = \min_{\alpha(t), s(t)} \int_0^{t_{\mathrm{f}}} w_{\mathrm{T}} + w_{\mathrm{E}} q_1 + w_{\mathrm{D}} \alpha q_{\mathrm{p}} \, \mathrm{d}t \tag{25a}$$

$$\text{s.t. } (23), \tag{25b}$$

$$V_{\mathrm{T}}(0) = V_0 - V_{\mathrm{L}}, \tag{25c}$$

$$c_{\mathrm{T},i}(0) = c_{i,0}, \quad i = 1, 2, \tag{25d}$$

$$c_{\mathrm{L},i}(0) = c_{i,0}, \quad i = 1, 2, \tag{25e}$$

$$c_{i,\mathrm{f}} V_{\mathrm{f}} = c_{\mathrm{T},i}(t_{\mathrm{f}})\, V_{\mathrm{T}}(t_{\mathrm{f}}) + c_{\mathrm{L,i}}(t_{\mathrm{f}})\, V_{\mathrm{L}}, \quad i = 1, 2, \tag{25f}$$

$$\alpha(t) \in [0,\, \infty), s(t) \in [0,\, 1]. \tag{25g}$$

The non-negative weighting coefficients $w_{\mathrm{T}}, w_{\mathrm{E}}, w_{\mathrm{D}}$ represent the weight (or price) for a unit of processing time, processing power, and diluant consumption, respectively.

4.2.2 Problem Solution

The optimization problem (25) can be solved using optimal control theory Hull (2003); Paulen and Fikar (2016). The complexity of the model (23) implies the use of numerical methods to solve the problem (25). We apply CVP (Balsa-Canto et al., 2001; Goh and Teo, 1988) and OC (Biegler, 2007) approaches. The control variables $\alpha(t)$ and $s(t)$ are considered to be piece-wise constant (PWC) on time intervals of variable length.

The power consumption is closely related to overall volume treated by the feed pump P1. This can be minimized if two events are met: (i) return of the retentate to the feed tank should be as small as possible ($s = 0$) and (ii) minimization of the diluant consumption. Therefore, we can expect that the optimal power operation will be closely related to optimal diluant usage with total recirculation.

4.3 Optimal Control – Case Studies

We present two case studies here out of the three case studies presented in the thesis. These cases differ in permeate flow models, and demonstrate different aspects of optimization and optimal operation. We consider that the membrane is completely impermeable to the macro-solute. Therefore, its rejection coefficient is $R_1 = 1$. The micro-solute completely passes the membrane, thus $R_2 = 0$.

4.3.1 Limiting Flux Model

The aim is to process the solution of volume $0.105\,\mathrm{m}^3$ from the initial point $[c_{1,0}, c_{2,0}] = [10,\ 31.5]\,\mathrm{mol\,m}^{-3}$, to the final point $[c_{1,\mathrm{f}}, c_{2,\mathrm{f}}] = [100,\ 10]\,\mathrm{mol\,m}^{-3}$.

The limiting flux model as used in (5) for permeate flow is assumed

$$q_{\mathrm{p}} = kA \ln\left(\frac{c_{\mathrm{lim}}}{c_{\mathrm{L},1}}\right), \tag{26}$$

where the limiting concentration is $c_{\mathrm{lim}} = 319\,\mathrm{mol\,m^{-3}}$, mass transfer coefficient is $k = 0.0172\,\mathrm{m\,h^{-1}}$, membrane area is $A = 1\,\mathrm{m^2}$. The flow rate inside the loop taken from the ultrafiltration experimental data of Verasztó et al. (2013) is $q_{\mathrm{L}} = 0.25\,\mathrm{m^3\,h^{-1}}$ and the loop volume is $V_{\mathrm{L}} = 0.005\,\mathrm{m^3}$. The list of combinations of w_{T}, w_{E} and w_{D} used here is given as:

1. Minimum time scenario ($w_{\mathrm{T}} = 1$, $w_{\mathrm{E}} = 0$, and $w_{\mathrm{D}} = 0$).
2. Almost minimum time scenario ($w_{\mathrm{T}} = 1$, $w_{\mathrm{E}} = 0.4$, and $w_{\mathrm{D}} = 0$).
3. Multi-objective scenario ($w_{\mathrm{T}} = 0.39$, $w_{\mathrm{E}} = 1$, and $w_{\mathrm{D}} = 0$).
4. Almost minimum power scenario ($w_{\mathrm{T}} = 0.01$, $w_{\mathrm{E}} = 1$, and $w_{\mathrm{D}} = 0$).
5. Minimum power scenario ($w_{\mathrm{T}} = 0$, $w_{\mathrm{E}} = 1$, and $w_{\mathrm{D}} = 0$).
6. Minimum diluant scenario ($w_{\mathrm{T}} = 0$, $w_{\mathrm{E}} = 0$, and $w_{\mathrm{D}} = 1$).

The minimum time, minimum diluant, and minimum power scenarios can be considered as interesting extreme cases. The weighting coefficients for the almost minimum time and almost minimum power scenarios are chosen such that the respective quantity increases within 10% of the theoretical minimal value.

To have both objectives minimized, multi-objective scenario was implemented. The weights were chosen to have minimization of both objectives (time and power) equally, as much as possible (Fig. 11).

The theoretical results for optimal operation of batch open-loop configuration predict (Paulen and Fikar, 2016; Paulen et al., 2013, 2015) that it will consist of three step strategy of time-varying α with modes: C, CVD, and dilution: $\alpha = (0, 1, \infty)$. The switching concentration from C to CVD of the macro-solute, for minimum time scenario is given by $c_1 = c_{\mathrm{lim}}/\mathrm{e}$ and increases towards c_{lim} for minimum diluant/power problem.

Optimal operation was calculated numerically using the method of orthogonal collocations implemented in package Dynopt (Čižniar et al., 2005). Several values for number of optimized intervals (finite elements) were tried to reveal the structure of the optimal solution. It was found that three intervals were sufficient and the further increase of their number did not lead to any substantial improvement in optimal value of the cost function.

Fig. 8, 9, and 10 show optimal total concentration (c_1, c_2) trajectories and optimal profiles of manipulated variables, α and s, respectively, for different considered scenarios. Green circle and red cross in concentration trajectories denote the initial and final concentration points, respectively.

The results confirm an agreement of the trajectory of concentrations and diluant rate α with the batch open-loop configuration.

The trajectory of control input s is shown in Fig. 10. As the dilution (last) step is performed after the process has been stopped, the control s is not optimized during it. If the objective is to minimize the batch time, s is 1 and thus the process reduces to a pure batch open-loop. On the other side, if the sole objective is to minimize energy, the recycle valve is fully open $(s = 0)$ all the time.

The optimal values of recirculation ratio s for the first and second step decrease as the objective of minimization moves from time minimization to power minimization. Note also that the power and diluant consumption minimization scenarios coincide, as it was predicted above.

The results of optimal control obtained coincide with the logic of respective minimizations. As seen in concentration diagram, the switching towards CVD mode for power minimization occurs later than in time minimization case, so as to reduce the volume of diluant needed to be pumped. The switching concentration and duration of CVD/VVD mode (diluant pumped) have an inverse relation based on the condition $c_1/c_2 = c_{1,\mathrm{f}}/c_{2,\mathrm{f}}$. If C mode is longer, the CVD mode is shorter and vice versa. As C mode is longer, lower reduction in micro-solute is required to achieve $c_1/c_2 = c_{1,\mathrm{f}}/c_{2,\mathrm{f}}$ during CVD mode, and hence lower volume of diluant is consumed.

The recycle valve is completely open $(s = 0)$ towards the loop and closed towards the tank for power minimization, in order for the feed pump to have the least volume to be pumped.

Table 4 shows a comparison of partial processing costs $\mathcal{J}_\mathrm{T}, \mathcal{J}_\mathrm{D}, \mathcal{J}_\mathrm{P}$ ((7)–(24)) using different scenarios. We can observe that the processing time and power are opposing objectives and cannot be minimized simultaneously. Minimum value of one of them results in maximum value of the other one.

The almost minimum time gave similar results to minimum time scenario

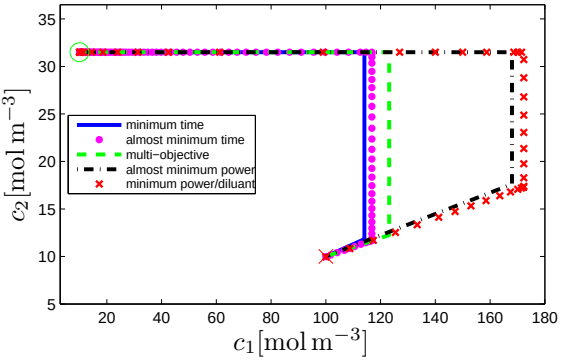

Figure 8: Evolution of component (c_1 and c_2) total concentrations for different scenarios.

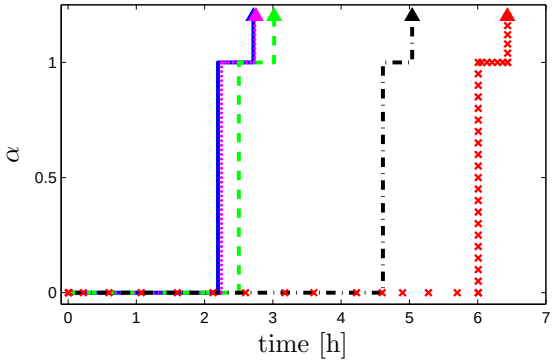

Figure 9: Optimal values of control α for different scenarios.

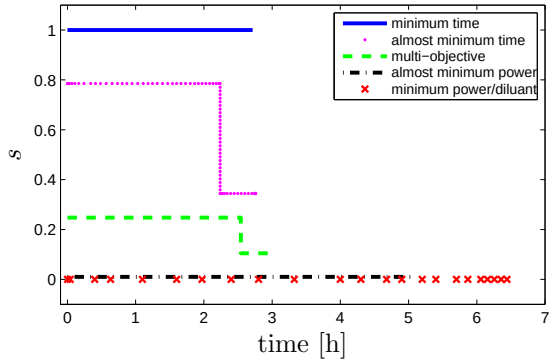

Figure 10: Optimal values of control s for different scenarios.

Table 4: Comparison of total processing time, volume needed to be pumped, and diluant consumption for different scenarios.

Scenario	w_T [€ h^{-1}]	w_E [€h m^{-3}]	w_D [€h m^{-3}]	$\mathcal{J}_T$ [h]	$\mathcal{J}_P$ [m^3]	$\mathcal{J}_D$ [m^3]
Min. time	1	0	0	2.71	0.6797	0.0103
Almost min. time	1	0.4	0	2.76	0.5108	0.0101
Multi-objective	0.39	1	0	3.02	0.2473	0.0095
Almost min. power	0.01	1	0	5.05	0.1116	0.0077
Min. power	0	1	0	6.46	0.1021	0.0076
Min. diluant	0	0	1	6.46	0.1021	0.0076

as seen in Table 4, and almost minimum power also gave similar results to minimum power scenario. The volume needed to be pumped did not increase substantially (9%) but the process time is reduced by 1.41 hours (20% reduction).

The Pareto front representation of the relation between these opposing objectives, i.e. time and power is depicted in Fig. 11. It can be observed that reduction of the power required is achieved at the expense of processing time, and vice versa. The utopia point (marked as hexagon) would be the perfect result for both objectives. Practically, however, it is not possible to have minimum of both objectives. Hence, a multi-objective optimal scenario located between both of them could be a good option.

With minimum power and time being extreme points, more realistic strategies are denoted by almost minimum scenarios. Thus, almost minimum time does not change the processing time much but greatly reduces the power (and diluant consumption). The same holds for the almost minimum power where the processing time is much reduced with only a slight increase of power needed. This is documented in both Table 4 and Fig. 11.

Let us now consider the situation when the final concentration of the macro-solute is increased to 170 mol m^{-3}. The theoretical results for time-optimal operation of batch open-loop configuration predict (Paulen and Fikar,

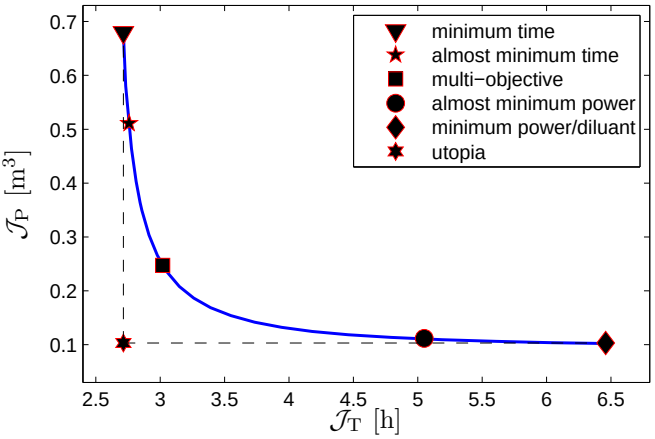

Figure 11: Pareto front diagram to depict the relation between optimized results, when moving from minimum time to minimum power.

2016; Paulen et al., 2013, 2015) that it will consist of a three-step strategy of time-varying α with modes: C, CVD, and C: $\alpha = (0, 1, 0)$ with the same switching concentration as before.

Optimal operation was calculated numerically using both the method of orthogonal collocations as well as control vector parametrization. The results confirm the observation from the first simulation part and are not repeated here.

We have also studied the effect of parametrization of the recirculation ratio s, and its effect on the final value of the cost function. We have found that the optimum is not particularly sensitive to s – if constant value is assumed over the whole processing time, the cost function increases by less than 1%. This is perfectly adequate in industrial conditions.

4.3.2 Separation of Lactose and Proteins

A case study taken from Rajagopalan and Cheryan (1991) is solved here where lactose is separated from proteins using ultrafiltration. The permeate flow rate model can be described as follows:

$$q_{\mathrm{p}}(c_{\mathrm{L},1}, c_{\mathrm{L},2}) = 63.42 - 12.439 \ln c_{\mathrm{L},1} - 7.836 \ln c_{\mathrm{L},2}, \tag{27}$$

where $c_{\mathrm{L},1}$ represents the concentration of proteins in the loop and $c_{\mathrm{L},2}$ represents the concentration of lactose in the loop. The aim is to process the solution of a volume 104 dL from the initial point $[c_{1,0}, c_{2,0}] = [3.3,\ 5.5]\,\mathrm{g\,dL^{-1}}$ to the final point $[c_{1,\mathrm{f}}, c_{2,\mathrm{f}}] = [9.04,\ 0.64]\,\mathrm{g\,dL^{-1}}$. The process parameters are the flow rate inside the loop $q_{\mathrm{L}} = 400\,\mathrm{dL\,h^{-1}}$ and the loop volume $V_{\mathrm{L}} = 4\,\mathrm{dL}$.

We study again different scenarios with the following weights:

1. Minimum time scenario ($w_{\mathrm{T}} = 1$, $w_{\mathrm{E}} = 0$, and $w_{\mathrm{D}} = 0$).
2. Almost minimum power scenario ($w_{\mathrm{T}} = 0.23$, $w_{\mathrm{E}} = 0.77$, and $w_{\mathrm{D}} = 0$).
3. Minimum power scenario ($w_{\mathrm{T}} = 0$, $w_{\mathrm{E}} = 1$, and $w_{\mathrm{D}} = 0$).
4. Minimum diluant scenario ($w_{\mathrm{T}} = 0$, $w_{\mathrm{E}} = 0$, and $w_{\mathrm{D}} = 1$).

The theoretical results for optimal operation of batch open-loop configuration suggest (Paulen and Fikar, 2016; Paulen et al., 2012, 2015) that it will consist of the three-step strategy of time-varying α with modes: C, VVD, and dilution: $\alpha = (0, 0.61, \infty)$.

Numerical optimization with the minimum power/diluant scenario gave the same and practically non-feasible solutions. The optimal operation occurs with $q_{\mathrm{p}} \to 0$ and takes infinite time to reach the desired concentrations (Table 5). Hence, the reason to implement almost minimum power scenario is to minimize power but in a practically feasible fashion. Otherwise, the results in Table 5 are consistent with the previous case.

Numerical diluant strategy of α agrees with the theory and the results for scenarios 1 and 2 are shown in Figs. 12, 13, and 14. Green circle and red cross in concentration trajectories denote the initial and final concentration points, respectively. The recirculation ratio s for the minimum time scenario is equal to one and for the almost minimum power is almost zero.

As inferred in the previous case study, to minimize power/diluant, the C mode takes longer than the C mode of time minimization scenario (Fig. 13). Again, it follows from the inverse relation between the switching concentration and the end point of the CVD/VVD mode. The switching to VVD mode is at higher concentration resulting in reduction of diluant consumption (during VVD) to meet the condition $c_1/c_2 = c_{1,\mathrm{f}}/c_{2,\mathrm{f}}$.

This can also be comprehended in the sense of volume in the system. As C mode gets longer, the volume gets lower and macro-solute concentration increases while micro-solute concentration stays constant. Hence lower volume of diluant is needed to be pumped to reduce the same concentration of micro-solute, but for a lower volume of feed (solution remaining in the process after C mode).

Similar to previous case, due to $s \approx 0$ in almost minimum power scenario (14), the time taken by VVD mode is longer than the time taken by VVD mode of minimum time scenario. The other reason for the longer time duration of VVD step in minimum power scenario is the lower permeate flux due to higher concentration of macro-solute (c_1) reached during C mode.

It can been studied from Table 5 that the difference in power consumption is quite large when the minimum time and the almost minimum power scenarios are compared. To investigate the main source of power reduction, we have simulated the process with optimal α from the almost minimum power scenario but in open-loop strategy ($s = 1$) and assuming identical initial and final concentrations.

The processing time was close to the minimum time scenario but the power consumption was similar to the one for the minimum time case. Hence, optimization of solely α will not lead to significant power reduction. The recirculation ratio s is the decisive factor, and needs to be optimized when power minimization is a part of the objective.

Table 5: Separation of lactose from proteins: comparison of individual cost functions for different scenarios.

Operation	w_T [€ h^{-1}]	w_E [€ h dL^{-1}]	w_D [€ h dL^{-1}]	$\mathcal{J}_T$ [h]	$\mathcal{J}_P$ [dL]	$\mathcal{J}_D$ [dL]
Min. time	1	0	0	4.65	1860	50
Almost min. power	0.23	0.77	0	26.8	112	38
Min. power	0	1	0	165.2	107.8	37
Min. diluant	0	0	1	165.2	107.8	37

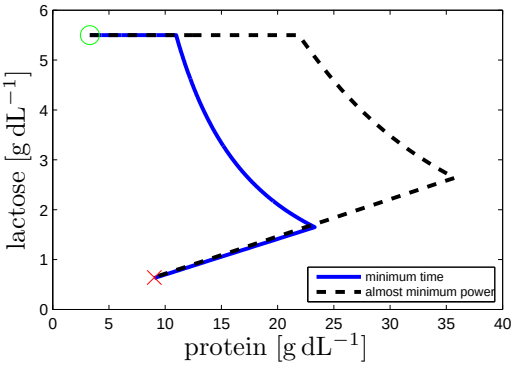

Figure 12: Separation of lactose from proteins: total concentration diagram.

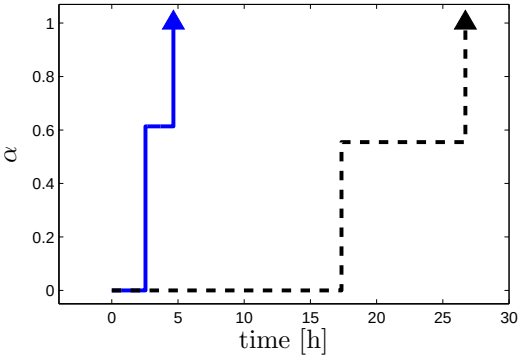

Figure 13: Separation of lactose from proteins: optimal values of control α.

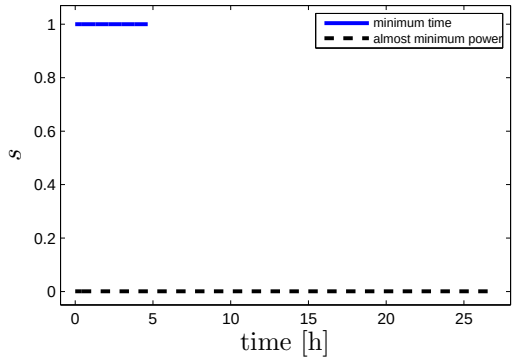

Figure 14: Separation of lactose from proteins: optimal values of control s.

5 Conclusions

In this thesis investigation of optimal operation of batch diafiltration membrane processes has been researched. The summary of thesis contributions:

1. Modeling of batch (open-loop) and batch with recirculation (closed-loop) types of membrane diafiltration processes.

2. Comparison of these two types of diafiltration configurations based on economical benefits they bring to separation.

3. Modeling of filtration rates using experimental data.

4. Optimal operation of batch open-loop DF was proposed using Pontryagin's minimum principle to find the optimal diluant addition rate. It was experimentally verified using the experimental filtration models estimated. The numerical optimization was performed for batch closed-loop DF to find the optimal diluant addition rate and recirculation ratio. Case studies were performed to study the optimal operation for both batch configurations.

The results based on the previous findings, and on this research work showed that the optimal operation consists of a three step strategy for both open-loop and closed-loop batch configurations. To be precise, three piece-wise constant inputs were found to satisfy the optimization objectives. The first and the last step use either pure filtration or pure dilution and the middle step is characterized by staying on singular surface where singular control is applied.

Experimental results of case studies for batch open-loop NDF to remove salt and concentrate lactose proved that optimal strategies improve the economics by reducing both processing time and diluant consumption, when compared to classical industrial strategies. In addition, the implementation of these optimal strategies does not require any alteration in current hardware and software setup in industries.

Numerical optimization results of case studies for closed-loop batch DF showed that power and diluant minimizations are equivalent. The same set

of optimal controls can be implemented to minimize diluant and power consumption. Time minimization on the other hand was achieved on the expense of higher diluant and power consumption.

The comparison of open-loop and closed-loop batch DF was done based on optimization results of case studies. It was concluded that for time minimization, recirculation is not required, only open-loop batch DF is enough. The configuration with possibility of partial recirculation (closed-loop) is useful when power minimization is a part of our optimal control problem.

Future work motivation can be summarized in the following items

- Online model estimation: In this research the model was estimated parameters were optimally obtained from process data, offline. Then this model was used to find the optimal strategy offline, followed by its implementation on plant. The future work will be to estimate the model parameters online, calculate the optimal strategy and steer the experiment optimally based on these online calculations, i.e. real-time optimal strategy implementation.

- Membrane types: The optimal operation experimental verification done was based on nanodiafiltration of lactose and salt solution. As this optimal operation theory is universal for all batch diafiltration processes, it would be interesting in future to verify it with other membranes, and for other solutes.

- Rejection coefficients: In current research the rejection of lactose and NaCl by the membrane was considered to be constant. In future, the optimal strategy could be designed and implemented considering these rejection coefficients as functions of concentrations.

- Experiments – partial recirculation: The experimental verification of the optimal control strategy designed and simulated in current work for batch closed-loop diafiltration.

Author's Publications

Thesis Related

Journals

1. A. Sharma, M. Jelemenský, R. Paulen, M. Fikar. Modeling and optimal operation of batch closed-loop diafiltration processes. *Chemical Engineering Research and Design*, vol. 122, pp. 198-210, 2017.

2. A. Sharma, R. Valo, M. Kalúz, R. Paulen, M. Fikar. Implementation of Optimal Strategy to Economically Improve Batch Membrane Separation. *Journal of Process Control*, vol. 76, pp. 155-164, 2019.

Conferences

1. A. Sharma, M. Jelemenský, R. Paulen, and M. Fikar. Modeling and Optimal Control of Membrane Process with Partial Recirculation. In *20th International Conference on Process Control*, Slovak Chemical Library, Štrbské Pleso, Slovakia, pp. 90–95, 2015.

2. A. Sharma, M. Jelemenský, R. Valo, M. Kalúz, M. Fikar. Process Control Education using a Laboratory Separation Process. In *11th IFAC Symposium on Advances in Control Education*, vol. 11, pp. 4–9, 2016.

3. A. Sharma, M. Jelemenský, R. Paulen, M. Fikar. Estimation of membrane fouling parameters for concentrating lactose using nanofiltration. In *26th European Symposium on Computer Aided Process Engineering*, Elsevier B.V, Slovenia, vol. 26, pp. 151–156, 2016.

4. A. Sharma, M. Jelemenský, R. Paulen, M. Fikar. Optimal Operation of Nanofilter Based Diafiltration Processes Using Experimental Permeation Models. In *21th International Conference on Process Control*, Slovak Chemical Library, Štrbské Pleso, Slovakia, pp. 185-190, 2017.

5. A. Sharma, R. Valo, M. Kalúz, R. Paulen, M. Fikar. Experimental validation and comparison of time-optimal and industrial strategy for

membrane separation process. In *9th Vienna International Conference on Mathematical Modeling*, Austria, 2018, pp. 869–874, 2018.

6. R. Paulen, A. Sharma, M. Fikar. Dynamic Real-time Optimization of Batch Membrane Processes using Pontryagin's Minimum Principle. In *28th European Symposium on Computer Aided Process Engineering*, Elsevier, vol. 28, pp. 1045–1050, 2018.

Other Publications

Journals

1. M. Jelemenský, A. Sharma, R. Paulen, M. Fikar. Time-optimal control of diafiltration processes in the presence of membrane fouling. *Computers & Chemical Engineering*, vol. 91, pp. 343–351, 2016.

2. A. Sharma, M. Fikar, M. Bakošová. Comparative study of Time Optimal Controller with PID Controller for a Continuous Stirred Tank Reactor. *Acta Chimica Slovaca*, no. 1, vol. 8, pp. 27–33, 2015.

Conferences

1. B. Verasztó, A. Sharma, Q. D. Nguyen, Gy. Vatai, P. Czermak, Z. Kovács: Membrane filtration technology for processing whey and converting whey-based lactose into galactooligosaccharides. In *Proceeding of the 6th Membrane Conference of Visegrad Countries*, E5 Warsaw, Poland: Polish Membrane Society, 2013.

2. M. Jelemenský, A. Sharma, R. Paulen, M. Fikar. Time-optimal Operation of Diafiltration Processes in the Presence of Fouling. In *12th International Symposium on Process Systems Engineering And 25th European Symposium on Computer Aided Process Engineering*, Elsevier B.V, Copenhagen, Denmark, pp. 1577–1582, 2015.

3. M. Jelemenský, A. Sharma, R. Paulen, M. Fikar. Multi-Objective Optimization of Batch Dialfiltration Processes in the Presence of Membrane Fouling. In *Proceedings of the 20th International Conference on Process*

Control, Slovak Chemical Library, Štrbské Pleso, Slovakia, pp. 84–89, 2015.

4. A. Sharma, J. Drgoňa, D. Ingole, J. Holaza, R. Valo, S. Koniar, M. Kvasnica. Teaching Classical and Advanced Control of Binary Distillation Column. In *11th IFAC Symposium on Advances in Control Education*, vol. 11, pp. 348–353, 2016.

Resumé

V tejto dizertačnej práci sa zaoberáme optimálnym riadením vsádzkových diafiltračných membránových procesov. Membránové procesy majú široké uplatnenie v chemickom, potravinárskom a farmaceutickom priemysle a taktiež pri spracovaní odpadových vôd v prakticky všetkých druhoch priemyselnej výroby. Princíp membránovej separácie je založený na veľkosti molekúl rôznych zložiek roztokov. Diafiltrácia je frakčná metóda, ktorá využíva externé rozpúšťadlo spolu s rôznymi technikami membránovej separácie (napr. ultrafiltrácia, nanofiltrácia, mikrofiltrácia a reverzná osmóza) za účelom zníženia obsahu nečistôt (napr. solí) a na zvýšenie koncentrácie produktu (napr. proteínov enzýmov alebo farbív) v roztoku.

V rámci práce skúmame vsádzkové diafiltračné membránové procesy bez recirkulácie (open-loop) a s recirkuláciou (closed-loop). V oboch prípadoch predpokladáme, že celý proces pracuje pri konštantnom tlaku a konštantnej teplote. Počiatočný roztok sa pridá do nádrže a dodáva sa na membránu pomocou čerpadla. Membrána je navrhnutá tak, aby zadržala látky s veľkou molekulovou veľkosťou (makrozložka) a umožnila prechod menších častíc (mikrozložky) cez membránu. Časť roztoku, ktorá je zadržaná membránou (retentát), je privádzaná späť do nádrže. Časť, ktorá prechádza cez membránu a je vypustená zo systému, sa nazýva permeát.

Riadiacou premennou pre diafiltračné procesy je množstvo pridávaného rozpúšťadla (najčastejšie voda) a definovaného pomerom α medzi vstupným tokom rozpúšťadla a výstupným tokom permeátu. Existuje niekoľko tradičných módov, ktoré sú odlišné v hodnote α. Najznámejšie takéto módy sú

- koncentračný mód ($\alpha = 0$)
- diafiltračný mód s konštantným objemom $\alpha = 1$,
- diafiltrácia s klesajúcim objemom $\alpha = (0, 1)$,
- mód riedenia $\alpha = \infty$.

V prípade diafiltrácie s recirkuláciou je prítomná ďalšia riadiaca veličina, t.j. recirkulačný pomer (s). Môže sa pohybovať medzi $0-1$ a reprezentuje deliaci

faktor medzi nádržou a obehom. $s = 0$ znamená, že žiadna látka sa nevracia do nádrže, zatiaľ čo $s = 1$ znamená úplný návrat do nádrže. $0 < s < 1$ znamená čiastočnú recirkuláciu.

Hlavným cieľom membránovej separácie je dosiahnuť požadovanú koncentráciu produktu a nečistôt. V tejto práci sa snažíme je dosiahnuť tento cieľ a zároveň minimalizovať produkčné náklady. Pri membránových separačných procesoch existuje niekoľko druhov optimalizačných funkcií, ktoré poznáme, ako napríklad: minimalizácia času, minimalizácia spotreby rozpúšťadla a minimalizácia spotreby energie.

V prípade vsádzkovej diafiltrácie bez recirkulácie bola hlavným cieľom tejto práce implementácia stratégie optimálneho riadenia vyvinutého našou skupinou na laboratórnej membránovej separačnej stanici. Táto stratégia bola analyticky odvodená pomocou Pontrjaginovho princípu minima a je možné ju nájsť jej podrobný popis v Paulen and Fikar (2016). Základné parametre implementácie boli nasledovné:

1. Všetky koncentrácie sa môžu merať kedykoľvek bez toho, aby bolo potrebné vzorky uchovať.

2. Teplota a tlak môžu byť regulované na úrovni konštantnej žiadanej hodnoty.

3. Bezpečnostné opatrenia sú implementované tak, aby automaticky upravovali alebo dokonca zastavili proces pri dosiahnutí nebezpečných úrovní hodnôt.

4. Zariadenie môže byť ovládané na diaľku.

5. Všetky merania sa ukladajú a uchovávajú v pravidelných časových intervaloch.

6. Počas experimentov je možné implementovať analyticky nájdenú stratégiu riadenia.

Vyššie uvedené otázky boli riešené riadením zariadenia cez PLC pomocou Matlab a WinCC HMI.

Ďalším dosiahnutým cieľom bolo nájdenie vhodných prietokových modelov, ktoré sa hodia pre experimenty vykonané na tejto stanici. Tento cieľ bol dosiahnutý vykonaním dynamického prispôsobenia modelov uvedených v odbornej literatúre experimentálnym údajom.

Po príprave zariadenia a získaní uspokojivých parametrizovaných prietokových modelov bolo d'alším cieľom vykonať a otestovať optimálnu stratégiu riadenia. Experimentálne sme uskutočnili niekoľko prípadových štúdií, ktoré sme následne porovnali s klasickými priemyselnými stratégiami na minimalizáciu času spracovania, minimalizáciu spotreby rozpúšťadla a váženej kombinácie oboch prístupov.

V prípade vsádzkovej diafiltrácie s recirkuláciou sme v odborej literatúre nenašli žiadnu podrobnú štúdiu týkajúcu sa matematického modelovania a riadenia pre tento spôsob filtrácie. Prvým krokom bolo teda rozsiahle štúdium dostupnej literatúry. Potom sme uskutočnili matematické modelovanie na základe materiálovej bilancie vstupov a výstupov zo systému. Takto odvodený model sme potom zjednodušili a skúmali sa aj jeho d'alšie varianty. Potom sme na nájdenie optimálnej stratégie použili numerické dynamické optimalizačné techniky za účelom minimalizácie spotreby času, minimalizácie spotreby rozpúšťadla, spotreby energie, alebo ich váženej kombinácie. Prípadové štúdie boli riešené pomocou simulácií za účelom štúdia výsledkov implementácie takejto optimálnej stratégie riadenia.

Závery boli vyvodené pre diafiltračné procesy. V prípade experimentálnej validácie optimálnej operácie pre diafiltráciu bez recirkulácie boli výsledky pozitívne. Optimálne stratégie boli lepšie ako klasické stratégie, ktoré sú v súčasnosti používané v priemysle. Úspešná bola aj optimalizácia riadenia diafiltrácie s recirkuláciou. Výsledky tiež naznačujú, že vsádzková diafiltrácia s recirkuláciou neprináša žiadne výhody (až na spotrebu energie) a môže byť nahradená klasickou vsádzkovou diafiltračnou konfiguráciou bez recirkulácie.

Bibliography

AWWA. Microfiltration and ultrafiltration membranes for drinking water - manual of water supply practices. American Water Works Association (AWWA), edition-1, 2005.

B. Balannec, M. Vourch, M. Rabiller-Baudry, and B. Chaufer. Comparative study of different nanofiltration and reverse osmosis membranes for dairy effluent treatment by dead-end filtration. *Separation and Purification Technology*, 42(2):195 – 200, 2005.

E. Balsa-Canto, J. R. Banga, A. A. Alonso, and V. S. Vassiliadis. Dynamic optimization of chemical and biochemical processes using restricted second-order information. *Computers and Chemical Engineering*, 25(4–6):539–546, 2001.

L. T. Biegler. An overview of simultaneous strategies for dynamic optimization. *Chemical Engineering and Processing*, 46:1043–1053, 2007.

M.R. Bilad, V. Discart, D. Vandamme, I. Foubert, K. Muylaert, and Ivo F.J. Vankelecom. Coupled cultivation and pre-harvesting of microalgae in a membrane photobioreactor (MPBR). *Bioresource Technology*, 155:410 – 417, 2014.

W. F. Blatt, A. Dravid, A. S. Michaels, and L. Nelsed. Solute polarization and cake formation in membrane ultrafiltration: Causes, consequences, and control techniques. *Membrane Science and Technology*, pages 47–91, 1970.

M. Cheryan. *Ultrafiltration and Microfiltration Handbook*. CRC Press, 1998.

M. Čižniar, M. Fikar, and M. A. Latifi. Matlab dynamic optimisation code dynopt. User's guide. Technical report, KIRP FCHPT STU Bratislava, Slovak Republic, 2005.

J. G. Crespo, K. W. Böddeker, and North Atlantic Treaty Organization. Scientific Affairs Division. *Membrane Processes in Separation and Purification*. Developments in Oncology. Springer, 1994.

Dow Water & Process Solutions. Filmtec reverse osmosis membranes technical manual. http://www.dow.com/scripts/litorder.asp?filepath=/609-00071.pdf.

G. Foley. Water usage in variable volume diafiltration: comparison with ultrafiltration and constant volume diafiltration. *Desalination*, 196:160 – 163, 2006.

C. J. Goh and K. L. Teo. Control parameterization: a unified approach to optimal control problems with general constraints. *Automatica*, 24(1):3–18, 1988.

D. G. Hull. *Optimal Control Theory for Applications*. Mechanical Engineering Series. Springer, 2003.

M. Y. Jaffrin and J. Ph. Charrier. Optimization of ultrafiltration and diafiltration processes for albumin production. *Journal of Membrane Science*, 97:71–81, 1994.

M. Jelemenský. *Optimal Control of Membrane Processes in the Presence of Fouling*. PhD thesis, ÚIAM FCHPT STU v Bratislave, 2016.

M. Jelemenský, A. Sharma, R. Paulen, and M. Fikar. Time-optimal operation of diafiltration processes in the presence of fouling. In *12th International Symposium on Process Systems Engineering And 25th European Symposium on Computer Aided Process Engineering*, pages 1577–1582, 2015a.

M. Jelemenský, A. Sharma, R. Paulen, and M. Fikar. Multi-objective optimization of batch dialfiltration processes in the presence of membrane fouling. In *Proceedings of the 20th International Conference on Process Control*, pages 84–89, 2015b.

M. Jelemenský, A. Sharma, R. Paulen, and M. Fikar. Time-optimal control of diafiltration processes in the presence of membrane fouling. *Computers & Chemical Engineering*, 91:343–351, 2016.

M. J. Jornitz and T. H. Meltzer. *Filtration and Purification in the Biopharmaceutical Industry, Second Edition*. Drugs and the Pharmaceutical Sciences. CRC Press (Taylor & Francis), 2007.

Z. Kovács, M. Fikar, and P. Czermak. Mathematical modeling of diafiltration. *Hungarian Journal of Industry and Chemistry*, 37, 2009.

H. Lutz. *Ultrafiltration for Bioprocessing*. Woodhead Publishing, 2015.

J. Mallevialle, P. E. Odendaal, AWWA Research Foundation, M.R. Wiesner, Lyonnaise des eaux Dumez (Firm), and South Africa. Water Research Commission. *Water Treatment Membrane Processes*. McGraw-Hill, 1996.

P. Ng, J. Lundblad, and G. Mitra. Optimization of solute separation by diafiltration. *Separation Science and Technology*, 11(5):499–502, 1976.

R. Paulen and M. Fikar. *Optimal Operation of Batch Membrane Processes*. Springer, 2016.

R. Paulen, M. Fikar, G. Foley, Z. Kovács, and P. Czermak. Optimal feeding strategy of diafiltration buffer in batch membrane processes. *Journal of Membrane Science*, 411-412:160–172, 2012.

R. Paulen, M. Jelemenský, M. Fikar, and Z. Kovács. Optimal balancing of temporal and buffer costs for ultrafiltration/diafiltration processes under limiting flux conditions. *Journal of Membrane Science*, 444(0):87 – 95, 2013.

R. Paulen, M. Jelemenský, Z. Kovács, and M. Fikar. Economically optimal batch diafiltration via analytical multi-objective optimal control. *Journal of Process Control*, 28:73–82, 2015.

L. S. Pontryagin, V. G. Boltyanskii, R. V. Gamkrelidze, and E. F. Mishchenko. *The Mathematical Theory of Optimal Processes*. John Wiley & Sons, Inc., New York, 1962.

N. Rajagopalan and M. Cheryan. Process optimization in ultrafiltration: Flux-time considerations in the purification of macromolecules. *Chemical Engineering Communications*, 106(1):57–69, 1991.

D. Rapaport. A membrane for all seasons. Environmental Protection, issue-07/01/2006, 2006.

A. Sharma, M. Jelemenský, R. Paulen, and M. Fikar. Modelling and optimal control of membrane process with partial recirculation. In *Proceedings of the 20th International Conference on Process Control*, pages 90–95, 2015.

A. Sharma, M. Jelemenský, R. Paulen, and M. Fikar. Estimation of membrane fouling parameters for concentrating lactose using nanofiltration. In *26th European Symposium on Computer Aided Process Engineering*, pages 151–156, 2016a.

A. Sharma, M. Jelemenský, R. Valo, M. Kalúz, and M. Fikar. Process control education using a laboratory separation process. In *Preprints of the 11th IFAC Symposium on Advances in Control Education*, pages 4–9, 2016b.

A. Sharma, M. Jelemenský, R. Paulen, and M. Fikar. Optimal operation of nanofilter based diafiltration processes using experimental permeation models. In *Proceedings of the 21st International Conference on Process Control*, pages 185–190, 2017a.

A. Sharma, M. Jelemenský, R. Paulen, and M. Fikar. Modeling and optimal operation of batch closed-loop diafiltration processes. *Chemical Engineering Research and Design*, 122:198–210, 2017b.

A. Sharma, R. Valo, M. Kalúz, R. Paulen, and M. Fikar. Experimental validation and comparison of time-optimal and industrial strategy for membrane separation process. In *Preprints of the 9th Vienna International Conference on Mathematical Modelling, Vienna, Austria, February 21-23, 2018*, pages 869–874, 2018.

A. Sharma, R. Valo, M. Kalúz, R. Paulen, and M. Fikar. Implementation of optimal strategy to economically improve batch membrane separation. *Journal of Process Control*, 76:155 – 164, 2019.

Synder. Nanofiltration membrane elements. Synder Sanitory Catalog 2014 - Synder Filtration, 2014.

A.Y. Tamime. *Membrane Processing: Dairy and Beverage Applications*. Wiley, 2012.

C. Y. Tang and J. O. Leckie. Membrane independent limiting flux for RO and NF membranes fouled by humic acid. *Environmental Science & Technology*, 41(13):4767–4773, 2007.

C. M. Todaro and H. C. Vogel. *Fermentation and Biochemical Engineering Handbook*. Elsevier Science, 2014.

B. Verasztó, A. Sharma, Q. D. Nguyen, Gy. Vatai, P. Czermak, and Z. Kovács. Membrane filtration technology for processing whey and converting whey-based lactose into galactooligosaccharides. In *Conference Proceeding of the 6th Membrane Conference of Visegrad Countries*, page E5, 2013.

S.H. Yalkowsky, Y. He, and P. Jain. *Handbook of Aqueous Solubility Data, Second Edition*. CRC Press, 2016.

L. J. Zeman. *Microfiltration and Ultrafiltration: Principles and Applications*. CRC Press (Taylor & Francis), 1996.